

RESEARCH ARTICLE

10.1002/2016JD025591

Key Points:

- Investigate the effects of mixed physical controls on soil moisture spatial variability at two different hydroclimate regions
- Develop the physically based hydrologic connectivity algorithm to better understand catchment hydrologic characteristics
- Improve parameterization of soil hydraulic properties using the physically based hydrologic connectivity in land surface modeling

Correspondence to:

B. P. Mohanty,
bmohanty@tamu.edu

Citation:

Kim, J., and B. P. Mohanty (2017), A physically based hydrological connectivity algorithm for describing spatial patterns of soil moisture in the unsaturated zone, *J. Geophys. Res. Atmos.*, 122, doi:10.1002/2016JD025591.

Received 28 JUN 2016

Accepted 27 JAN 2017

Accepted article online 1 FEB 2017

A physically based hydrological connectivity algorithm for describing spatial patterns of soil moisture in the unsaturated zone

Jonggun Kim¹  and Binayak P. Mohanty¹ 

¹Department of Biological and Agricultural Engineering, Texas A&M University, College Station, Texas, USA

Abstract Hydrologic connectivity has been proposed as an important concept for understanding local processes in the context of catchment hydrology. It can be useful for characterizing the soil moisture variability in complex heterogeneous landscapes. The current land surface models (e.g., Community Land Model, CLM) could not completely account for flow path continuity and connected patterns of subsurface properties in the unsaturated zone. In this study, we developed a physically based hydrologic connectivity algorithm based on dominant physical controls (e.g., topography, soil texture, and vegetation) to better understand the spatially distributed subsurface flow and improve the parameterization of soil hydraulic properties in hydrological modeling. We investigated the effects of mixed physical controls on soil moisture spatial variability and developed hydrologic connectivity using various thresholds. The connectivity was used for identifying the soil moisture variability and applied in a distributed land surface model (CLM) for calibrating soil hydraulic properties and improving model performance for estimating spatially distributed soil moisture. The proposed concept was tested in two watersheds (Little Washita in Oklahoma and Upper South Skunk in Iowa) comparing estimated soil moisture with the airborne remote sensing data (Electronically Scanning Thinned Array Radiometer and Polarimetric Scanning Radiometer). Our finding demonstrated that the spatial variations of soil moisture could be described well using physically based hydrologic connectivity, and the land surface model performance was improved by using the calibrated (distributed) soil hydraulic parameters. In addition, we found that the calibrated soil hydraulic parameters significantly affect model outputs not only on the water cycle but also on surface energy budgets.

1. Introduction

Recently, various studies have been conducted to understand catchment dynamics through the examination of catchments emergent properties (i.e., spatially connected patterns of flow paths or variable source areas) [Amoros and Bornette, 2002; Sivapalan, 2005; McDonnell *et al.*, 2007; Ali and Roy, 2009]. Hydrologic connectivity has been developed as an important concept for understanding local processes in the context of catchment hydrology. The connectivity can be defined as connected pathways of surface and subsurface flow and spatial patterns of soil moisture [Western *et al.*, 2001; Ali and Roy, 2010; Jencso and McGlynn, 2011]. It can also provide a missing linkage for preferential flow inferred from unexpected water and chemical migration, which cannot be successfully accounted for through the current parameterization and land surface modeling (LSM: Community Land Model (CLM), Noah Land Surface Model (Noah LSM), Variable Infiltration Capacity, etc.). Various connectivity metrics have been used in hydrology and ecology such as FRAGSTATS (e.g., cohesion, aggregation index (AI), and contagion) [McGarigal *et al.*, 2002], semivariogram range [Western *et al.*, 1998], gamma index [Ricotta *et al.*, 2000], directional connectivity index (DCI) [Larsen *et al.*, 2012], and integral connectivity scale (ICS) [Western *et al.*, 2001]. The connectivity metrics are useful to better understand catchment hydrologic characteristics and identify runoff source areas at the hillslope scale. The semivariogram range has the difficulty in interpreting the variation of parameters (e.g., nuggets, sills, and ranges) with respect to the direction. Common connectivity metrics (e.g., cohesion and AI) do not reflect the relative differences in connectivity, while DCI and ICS can describe the relative variability of spatially connected patterns across landscapes. Several studies explored the combined effects of topography and vegetation on connectivity of runoff source areas and shallow groundwater and showed the potential for improving the estimation of hydrologic connectivity [Mayor *et al.*, 2008; Hwang *et al.*, 2009; Emanuel *et al.*, 2014]. Jencso *et al.* [2009, 2010] derived the hydrologic connectivity between catchment landscapes and channel network to identify runoff source areas based on topographic characteristics. They explored the

linkage between catchment structure and runoff characteristics and defined the connectivity from flow path continuity across hillslope, riparian, and stream (HRS) interfaces. Using this concept, *Smith et al.* [2013] developed the catchment connectivity model to predict streamflow production using simulated hydrologic connectivity across HRS along a stream network. *Western et al.* [2004] demonstrated that saturation excess processes can be indicated by patterns of near-surface soil moisture used for developing hydrologic connectivity using the integral connectivity scale technique. Based on these studies, hydrologic connectivity demonstrated spatially connected patterns of landscape information such as wetness condition, streamflow, and surface characteristics (e.g., topography and vegetation).

In the past, soil moisture variability has been extensively studied at different spatial scales using in situ and remote sensing data in various hydroclimate regions. It is crucial for understanding hydrological processes and catchment characteristics across scales [*Gaur and Mohanty*, 2016]. The spatial variability of soil moisture can be a critical factor to develop the hydrologic connectivity characterizing spatial patterns of surface and subsurface flow. However, soil moisture information is very limited in deep soils as well as near-surface soils for large regions. Various studies have been performed to derive soil moisture and soil properties based on terrain indices in landscapes [*Moore et al.*, 1993; *Western et al.*, 1999; *Wilson et al.*, 2005; *Zhu and Lin*, 2010]. Soil moisture varies across space and time according to geophysical parameters (i.e., physical controls) such as topography, soil properties, and vegetation characteristics. The physical controls play a significant role in characterizing the heterogeneous landscape in surface and subsurface hydrology [*Famiglietti et al.*, 1999; *Mohanty and Skaggs*, 2001; *Joshi and Mohanty*, 2010]. *Gaur and Mohanty* [2013] explored the effects of physical controls on spatial patterns of soil moisture in humid and subhumid climatic regions. They identified the dominant physical controls that strongly affect the soil moisture variability at various scales. Spatial patterns of soil moisture are dependent on a set of various (dynamic and static) physical controls which have been defined as precipitation, topography, soil, and vegetation. Thus, the spatial distribution of mixed physical controls can be considered to develop hydrologic connectivity as landscape descriptors or potential predictors for redistribution of surface and subsurface flow. Since precipitation and vegetation vary temporally, dynamic hydrologic connectivity can be also developed using the temporal aspect of physical controls. Recently, *Kim and Mohanty* [2016] developed the hydrologic connectivity algorithm for lateral subsurface flow processes based on the dominant physical controls to improve hydrological modeling at a subwatershed scale. Their hydrologic connectivity based on the mixed physical controls (assuming that the variables have equal effects on hydrological processes) was successfully reflected to account for subsurface lateral flow processes in land surface modeling. However, the equal contributions of different physical controls for describing the soil moisture variability may not be applicable in other regions or spatiotemporal scales. Soil moisture variability may have different effects of dominant physical controls. Thus, it may be needed to investigate the effects of mixed (weighted) physical controls as well as the interactions between the controls on soil moisture distribution and subsurface flow.

In addition to improving the process modeling, hydrologic connectivity can be employed for improvement of existing parameterizations (especially for soil hydraulic properties) in land surface modeling. Land surface models estimate soil water content in soil profiles based on soil hydraulic properties which directly influence water holding capacity in the unsaturated zone [*Price et al.*, 2010]. In land surface modeling, soil hydraulic properties are typically derived from empirical equations as their default parameters such as the pedotransfer function by *Cosby et al.* [1984]. Although model parameter calibration is critical for achieving accurate model output, most land surface models use a set of default or spatially uniform model parameters [*Li et al.*, 2011]. The empirically derived default soil hydraulic parameters might not be enough to describe the soil moisture variability in spatially heterogeneous landscapes. Thus, in this study, we investigated the effects of mixed physical controls on soil moisture variability to develop physically based hydrologic connectivity and effectively calibrate the distributed soil hydraulic properties across large regions in land surface hydrological modeling.

The main objectives of this study are (1) to study spatially distributed patterns of mixed physical controls which govern soil water redistribution in the unsaturated zone, (2) to develop a physically based hydrological connectivity algorithm for better describing the spatial connection of subsurface flow in the unsaturated zone, and (3) to improve soil hydraulic parameterization schemes based on hydrologic connectivity in distributed hydrological modeling.

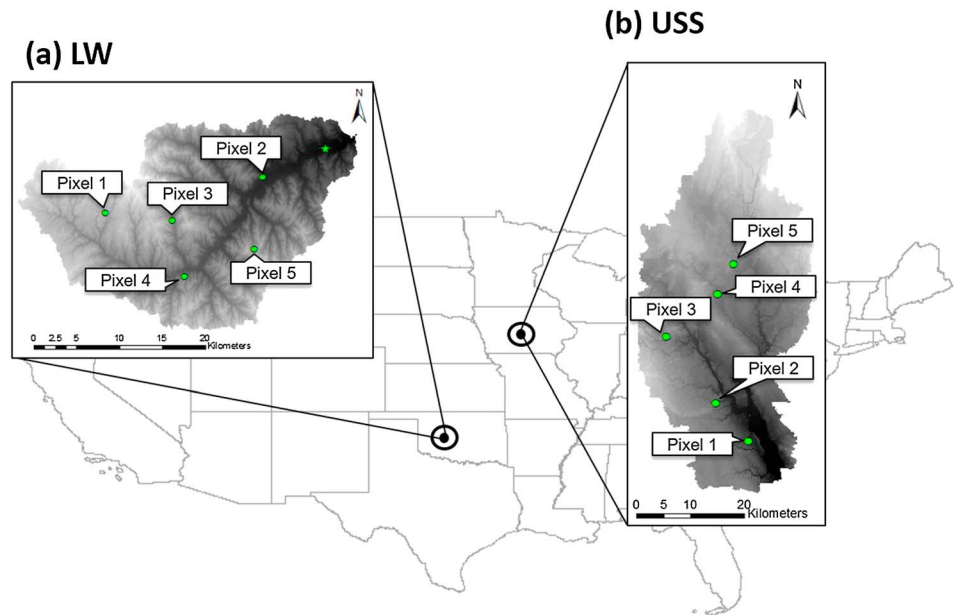


Figure 1. Study sites of (a) Little Washita (LW) in Oklahoma and (b) Upper South Skunk (USS) in IOWA. The pixels represent connected and unconnected regions selected for analysis.

2. Methodology

2.1. Study Sites

The Little Washita (LW) watershed in Oklahoma and Upper South Skunk (USS) watershed in Iowa were selected as the test sites for this study (Figure 1). The study sites have different hydroclimatic conditions and watershed characteristics (e.g., soil properties, land cover, and topography). The LW watershed is classified as subhumid climate with a mean annual rainfall of approximately 926 mm and temperature of 16°C. The LW region (area of about 600 km²) has rangeland and pastures dominated by patches of winter wheat and other crops and soil textures ranging from fine sand to silty loam across the watershed. Several field campaigns were conducted in this watershed such as Washita '94, Southern Great Plains 1997 (SGP97), Soil Moisture Experiments 2003 (SMEX03), and Cloud Land Surface Interaction Campaign 2007 (CLASIC07).

The climate of USS is humid with a mean annual rainfall of approximately 956 mm and temperature of 10.7°C. The region (area of about 2000 km²) has mostly agricultural crops such as corn and soybean and mainly silty clay loam. The Soil Moisture Experiments 2002 (SMEX02) and Soil Moisture Active Passive Vegetation Experiment 2012 (SMAPVEX12) field campaigns were conducted in this watershed. Our proposed approach was validated with Electronically Scanning Thin Array Radiometer (ESTAR) pixel-based (800 × 800 m) near-surface soil moisture products [Jackson *et al.*, 1999] obtained during SGP97 (18 June to 17 July 1997) for the LW watershed and Aircraft Polarimetric Scanning Radiometer (PSR [Bindlish and Jackson, 2002]) observed during SMEX02 (25 June to 12 July 2002) for the USS watershed. We selected several pixels on connected and unconnected regions with different characteristics and complexities (e.g., soil type, land use, and topography) as shown in Table 1 (Figure 1). On the selected pixels, the performance of land surface model was

Table 1. Characteristics of Selected Pixels in the Study Sites

	LW			USS		
	Elevation	Soil Texture	Land Use	Elevation	Soil Texture	Land Use
Pixel 1	418 m	Silty clay loam	Crop	314 m	Sandy clay loam	Crop
Pixel 2	338 m	Loam	Crop	294 m	Loam	Forest
Pixel 3	391 m	Sandy clay loam	Forage	321 m	Loam	Crop
Pixel 4	379 m	Sandy clay loam	Alfalfa	310 m	Clay loam	Grass
Pixel 5	398 m	Clay loam	Pasture	311 m	Loam	Crop

Table 2. Means and Standard Deviations for the Four Hydraulic Parameters for Various Textural Classes [From Cosby *et al.*, 1984, Table 3]

Class	b		Log ψ_{sat}		Log K_{sat}		θ_{sat}	
	Mean	SD	Mean	SD	Mean	SD	Mean	SD
Sandy loam	4.74	1.40	1.15	0.73	-0.13	0.67	43.4	8.8
Sand	2.79	1.38	0.84	0.56	0.82	0.39	33.9	7.3
Loamy sand	4.26	1.95	0.56	0.73	0.30	0.51	42.1	7.2
Loam	5.25	1.66	1.55	0.66	-0.32	0.63	43.9	7.4
Silty loam	5.33	1.72	1.88	0.38	-0.40	0.55	47.6	5.4
Sandy clay loam	6.77	3.39	1.13	1.04	-0.20	0.54	40.4	4.8
Clay loam	8.17	3.74	1.42	0.72	-0.46	0.59	46.5	5.4
Silty clay loam	8.72	4.33	1.79	0.58	-0.54	0.61	46.4	4.6
Sandy clay	10.73	1.54	0.99	0.56	0.01	0.33	40.6	3.2
Silty clay	10.39	4.27	1.51	0.84	-0.72	0.69	46.8	6.2
Light clay	11.55	3.93	1.67	0.59	-0.86	0.62	46.8	3.5

evaluated with and without the subsurface hydrologic connectivity for the study watersheds. In addition, the model performances were compared at various extent scales to evaluate the spatial variability of soil moisture prediction for large regions within the watersheds.

2.2. Land Surface Model (Community Land Model)

Community Land Model (CLM) serves as the dynamic land surface model component of the Community Earth System Model [Oleson *et al.*, 2010]. CLM consists of various processes such as biogeophysics, hydrologic cycle, biogeochemistry, and dynamic vegetation. The model estimates surface and subsurface runoff based on the simple TOPMODEL-based runoff (SIMTOP) [Niu *et al.*, 2005]. The SIMple Groundwater Model (SIMGM) [Niu *et al.*, 2007] is used for considering water table dynamics as the lower boundary. Bare soil evaporation and plant transpiration are calculated using the Philip and De Vries [1957] diffusion model and an aerodynamic approach which is based on the Biosphere-Atmosphere Transfer Scheme model [Dickinson *et al.*, 1993] and a stomatal resistance from the LSM model [Bonan, 1996]. CLM is coupled with the River Transport Model (RTM) for the runoff routing process [Oleson *et al.*, 2010]. The soil profile is divided into 10 soil layers with the fixed thickness of 1.75, 2.76, 4.55, 7.5, 12.36, 20.38, 33.60, 55.39, 91.33, and 113.7 cm (total depth of 343 cm). The soil water flow is solved by the modified Richards' equation (1) [Zeng and Decker, 2009] which is derived by subtracting the hydrostatic equilibrium soil moisture distribution from the original Richards' equation for improving the mass-conservative numerical scheme when the water table is within the soil column,

$$\frac{\partial \theta}{\partial t} = \frac{\partial}{\partial z} \left[K \left(\frac{\partial(\psi - \psi_e)}{\partial z} \right) \right] - Q \quad (1)$$

where ψ and ψ_e are the soil matric potential and equilibrium soil matric potential (cm), z is soil depth (cm) taken positive upward, K is hydraulic conductivity (cm d^{-1}), and Q is a soil moisture sink term, which is the root water extraction rate by plants. The hydraulic conductivity, equilibrium soil matric potential, and equilibrium volumetric water content are shown in equations 2–4 based on Clapp and Hornberger [1978],

$$K(\theta) = K_{\text{sat}} \left(\frac{\theta}{\theta_{\text{sat}}} \right)^{2b+3} \quad (2)$$

$$\psi_e = \psi_{\text{sat}} \left(\frac{\theta_e(z)}{\theta_{\text{sat}}} \right)^{-b} \quad (3)$$

$$\theta_e(z) = \theta_{\text{sat}} \left(\frac{\psi_{\text{sat}} + z\nabla - z}{\psi_{\text{sat}}} \right)^{-\frac{1}{b}} \quad (4)$$

where $K(\theta)$ and K_{sat} are the unsaturated and saturated hydraulic conductivity (cm d^{-1}), θ and θ_{sat} are the volumetric soil water content and saturated soil water content ($\text{cm}^3 \text{cm}^{-3}$), ψ_{sat} is the saturated soil matric potential (cm), $\theta_e(z)$ is the equilibrium (e) volumetric water content ($\text{cm}^3 \text{cm}^{-3}$) at depth z (z_v is the water table depth), and b is the curve fitting parameter related to the pore size distribution ($-$), respectively. Primarily, the four soil hydraulic properties (θ_{sat} , K_{sat} , ψ_{sat} , and b) are major input parameters for estimating soil

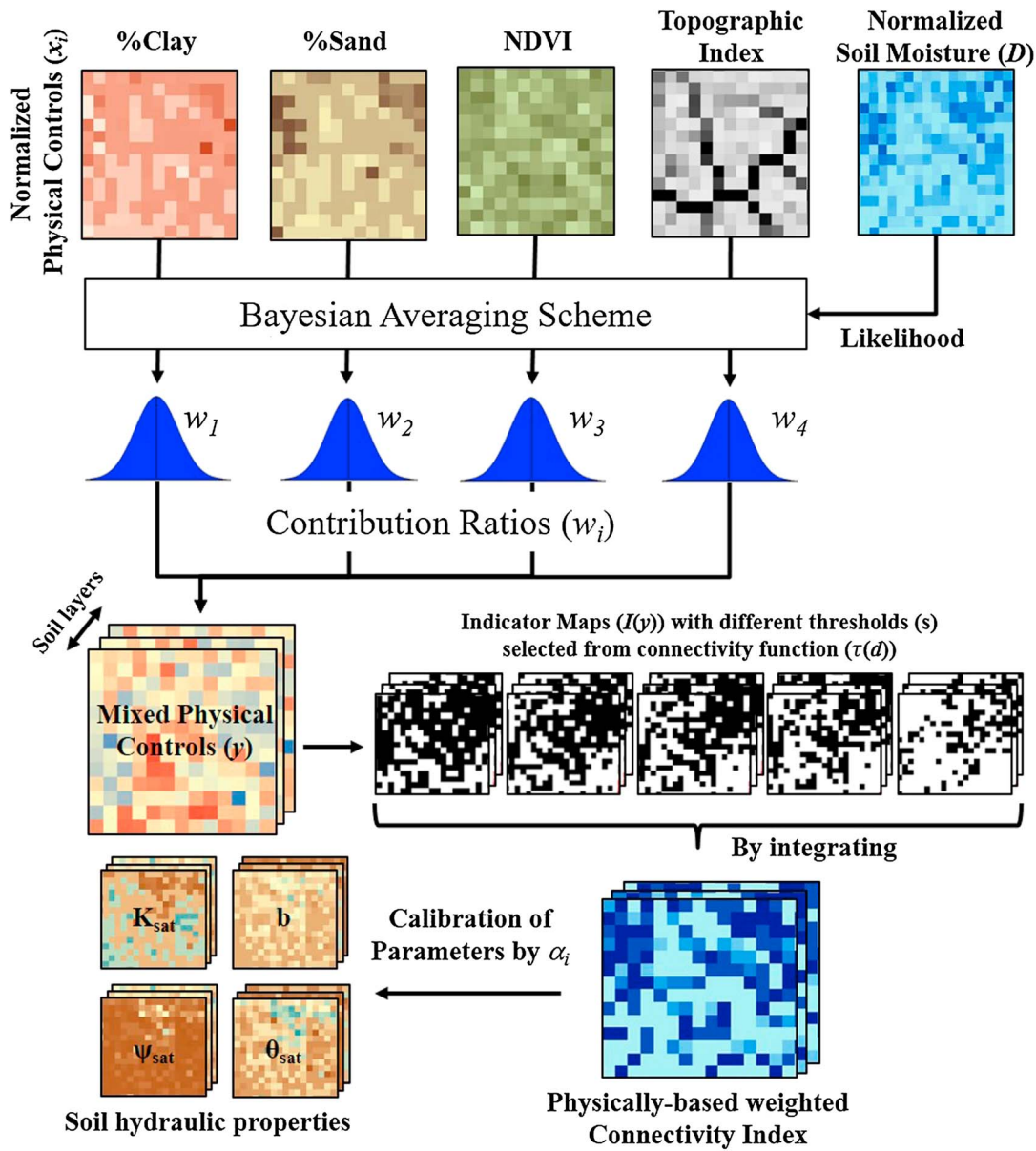


Figure 2. Schematic diagram of information flow for developing connectivity index using Bayesian averaging of dominant physical controls and calibrating distributed soil hydraulic parameters. α_i is the calibrating factor for each parameter based on their standard deviation that is determined by the physically based hydrologic connectivity index.

moisture distribution in CLM [Huang *et al.*, 2013]. These soil properties are calculated based on the work by Clapp and Hornberger [1978] and Cosby *et al.* [1984], which are determined according to percent sand and percent clay contents (equations 5–8) (called default parameters in this paper). The means and standard deviations of the parameters are available from Cosby *et al.* [1984] as shown in Table 2.

$$\theta_{sat} = 0.489 - 0.00126 \times \%sand \quad (5)$$

$$b = 2.91 + 0.159 \times \%clay \quad (6)$$

$$\psi_{sat} = 10 \times 10^{(1.88 - 0.0131 \times \%sand)} \quad (7)$$

$$K_{sat} = 0.0070556 \times 10^{(-0.884 + 0.0153 \times \%sand)} \quad (8)$$

After investigating the effects of mixed physical controls on soil moisture variability, the soil hydraulic parameters were calibrated using the physically based hydrologic connectivity algorithm developed in section 2.4

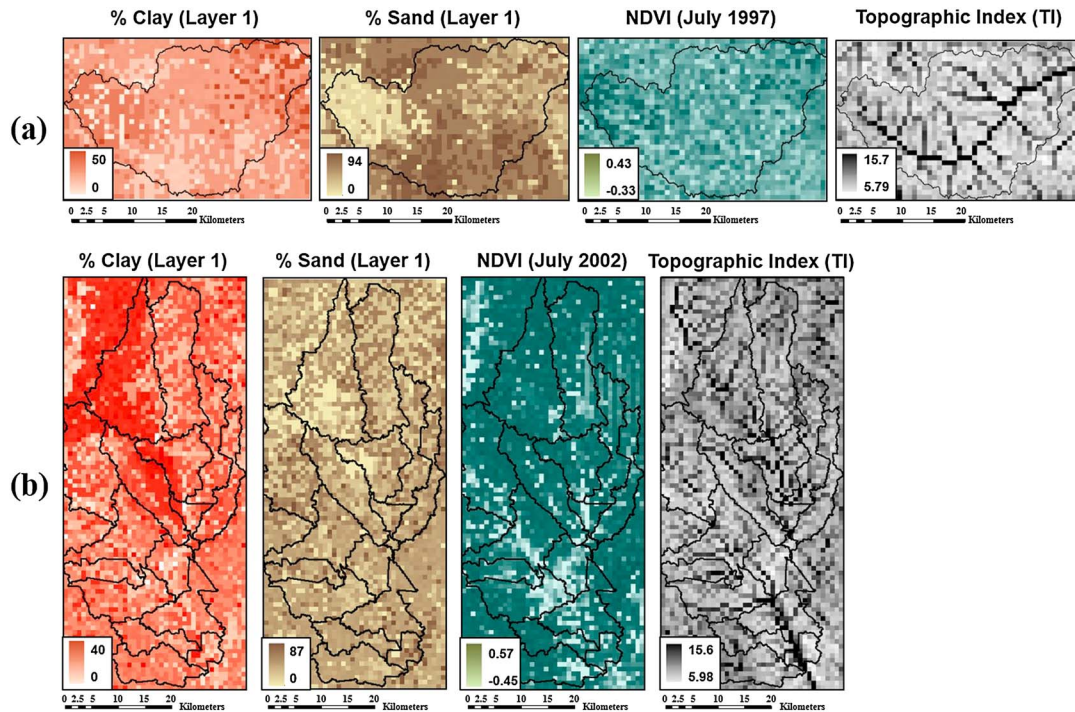


Figure 3. Dominant physical controls (soil texture, vegetation, and topography) for the (a) LW and (b) USS watersheds (spatial resolution of 800 m).

(Figure 2). To evaluate the land surface model performance, we compared the model outputs (e.g., soil water content, evapotranspiration, surface runoff, and water storage) estimated by using the default soil hydraulic parameters versus using the calibrated soil hydraulic parameters.

We used CLM4.0 loosely coupled with RTM in an offline mode with atmospheric forcing data (precipitation, temperature, specific humidity, wind speed, surface air pressure, and solar radiation) collected from the U.S. Department of Agriculture (USDA) Agricultural Research Service (ARS) Micronet network for the LW watershed and SMEX02 Rain Gauge network for the USS watershed. Model inputs for the two watersheds were generated at a spatial resolution of 800 m using land cover, soil types with depth, and topographic information obtained from NLCD (National Land Cover Database), SSURGO (Soil Survey Geographic database), and NED (National Elevation Dataset), respectively.

2.3. Mixed Physical Controls in Complex Landscapes

Kim and Mohanty [2016] developed hydrologic connectivity assuming that all physical controls are contributing equally to representing the soil moisture distribution in the unsaturated zone. However, that assumption has a limitation to be applied into other complex landscapes due to site-specific characteristics. In complex landscapes, spatial distribution of soil moisture varies and shifts with landscape characteristics such as spatial patterns of soils, vegetation, topography, and hydroclimates [Gaur and Mohanty, 2013, 2016]. To better characterize the spatial variability of soil moisture, the total contribution of various physical controls and their interactions need to be accounted. In this study, dominant physical controls (i.e., soil texture (%clay and %sand), topography (Topographic Index (TI), $\ln(a/\tan\beta)$), and vegetation (normalized difference vegetation index (NDVI), $(R_{NIR} - R_{red})/(R_{NIR} + R_{red})$) were considered. R_{NIR} and R_{red} are the reflectance of near-infrared (NIR) radiation and visible red radiation, respectively; a represents the upslope area; and $\tan\beta$ is the local downslope. Spatial data were collected from the Soil Survey (SSURGO), Landsat 5 imagery, and USDA-NRCS Geospatial Data Gateway for the two watersheds (Figure 3). To effectively estimate the contributing ratios (weights) for the physical controls and their interactions, we used the Bayesian averaging scheme [Hoetting et al., 1999] that can provide proper weights that show how the controls contribute to describing the spatial variability of soil moisture (equation (9)).

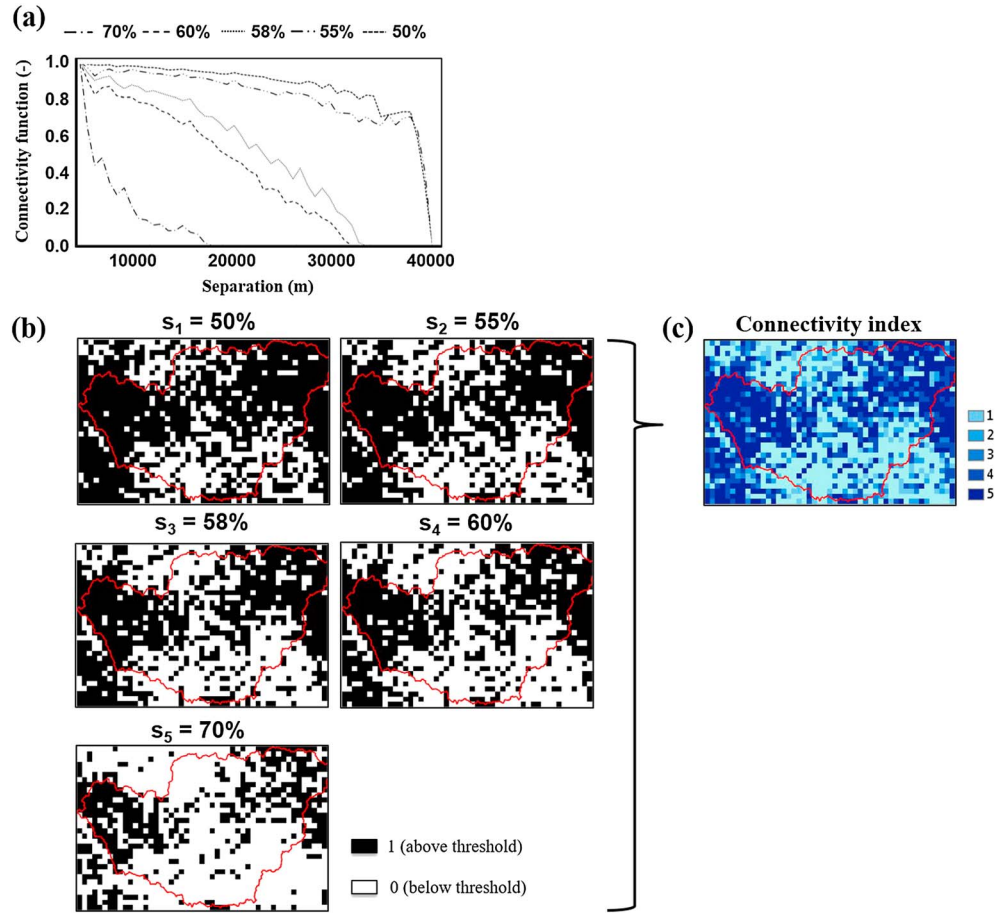


Figure 4. Physically based hydrologic connectivity: (a) connectivity functions ($\tau(d)$) calculated using indicator maps ($I(y)$) of mixed physical controls, (b) indicator maps for five selected thresholds (s_j), and (c) physically based hydrologic connectivity index map developed by integrating five indicator maps.

$$P(y|x_1, \dots, x_j) = \sum_{i=1}^j P_i(x_i|D)P_i(y|x_i, D) \quad (9)$$

where y is the combined (weighted) physical controls, x_i is the normalized physical controls ($i = 1, \dots, j$), j is the number of physical controls and interaction terms used, PDF ($P_i(x_i|D)$) is the posterior probability for physical controls given the normalized soil moisture measurements (D) and defined as contributing ratios (w_i) of normalized physical controls (x_1, x_2, x_3, x_4 as %clay, %sand, NDVI, and TI), and the conditional PDF ($P_i(y|x_i, D)$) represents the posterior distributions of y given physical controls and measurements. Interaction terms were also considered to examine the joint effects of physical controls (e.g., x_{1-2} , x_{1-3} , x_{1-4} , x_{2-3} , x_{2-4} , and x_{3-4}). In this study, the observed spatial patterns of soil moisture obtained from ESTAR and PSR for the LW and USS watersheds, respectively, were used to determine the contributions of physical controls. The estimated contributing ratios were used to combine the dominant controls and to develop the hydrologic connectivity for the study watershed.

2.4. Development of Physically Based Hydrologic Connectivity

By and large, hydrologic connectivity has been developed by patterns of wetness condition (e.g., soil moisture) or surface topography (e.g., contributing area) at a catchment scale [Western et al., 2001; Jencso and McGlynn, 2011]. However, information for surface wetness or root zone soil moisture is very sparse, and surface topography cannot sufficiently reflect the patterns of subsurface flow [Kim and Mohanty, 2016]. Thus, we developed physically based hydrologic connectivity using the mixed physical controls (i.e., %clay, %sand, NDVI, and TI) to identify the spatial variation of soil moisture. Hydrologic connectivity can be defined as

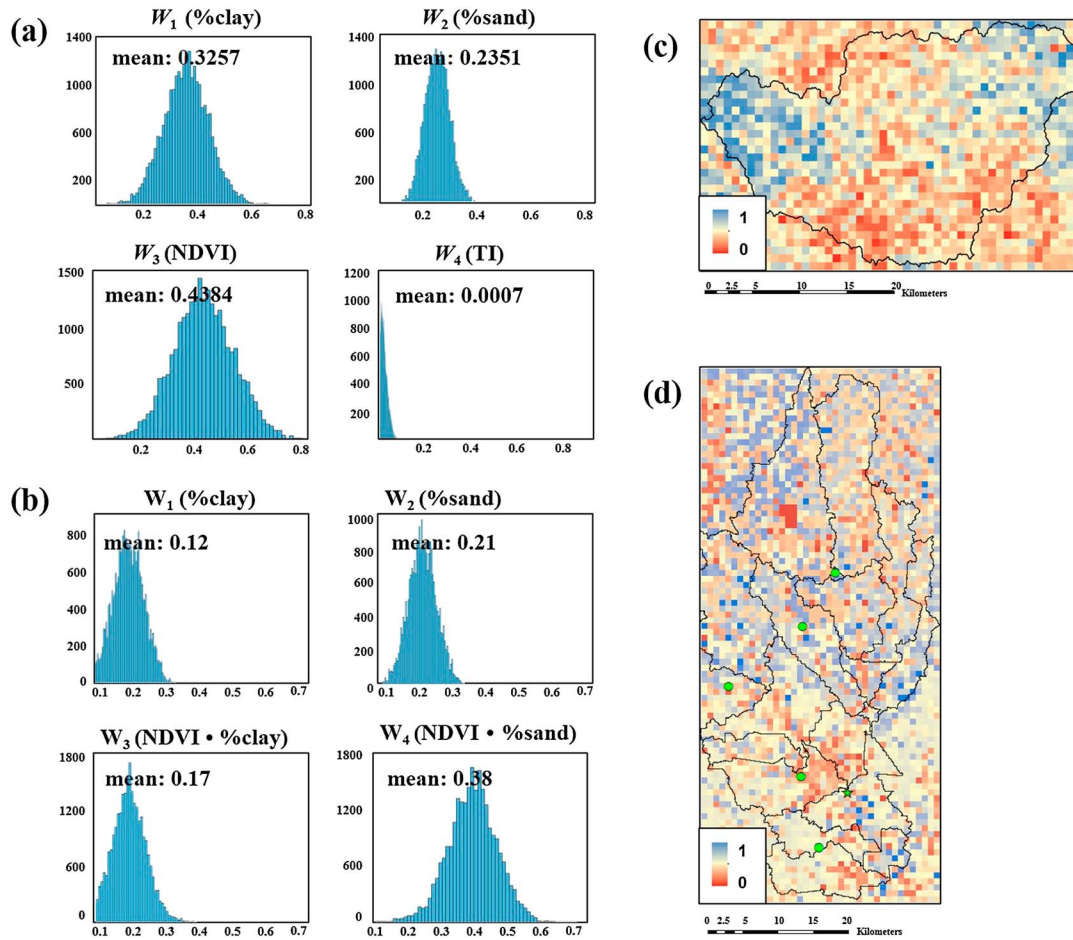


Figure 5. Contributing ratios (weights, w_j) of physical controls (a) for LW and (b) for USS and mixed (weighted) physical controls maps (c) for LW and (d) for USS.

spatial features which concentrate flow and reduce travel times [Knudby and Carrera, 2005], and it shows how cells are connected to each other across a domain under a certain threshold of interest variable. Among various connectivity metrics, we used the integral connectivity scale technique which was successfully tested in a previous study [Kim and Mohanty, 2016] to describe the soil moisture spatial variability. The indicator map (l) is used to describe the spatial patterns of interest variable (y , mixed physical controls) above a certain threshold (s) in the hydrologic connectivity process (10). Connectivity is calculated using the indicator map $l(y)$ and the connectivity function ($\tau(d)$) expressed as equation (11).

$$l(y) = \begin{cases} 0 & \text{if } y < s \\ 1 & \text{if } y \geq s \end{cases} \quad (10)$$

$$\tau(d) = P(h \leftrightarrow h + d | h, h + d \in H) \quad (11)$$

where h is a certain cell in a domain (H) and d is the distance between two cells.

Indicator maps ($l(y)$) for various thresholds (0–100%) were created using a mixed physical controls map generated with the contributing ratios of different physical controls. It shows that pixels above the thresholds on the mixed controls map were assigned to “1” and others assigned to “0.” To consider various connected patterns of mixed physical controls, we selected five representative thresholds from the connectivity functions ($\tau(d)$) that reflect the connectivity patterns well across the watershed (Figure 4a) [Western et al., 2001; Kim and Mohanty, 2016]. In this study, we manually selected the thresholds indicating the connected patterns in the connectivity function. Based on the various thresholds, it can be inferred how moisture can be drying or wetting spatially across the watersheds. In turn, the indicator maps for the five thresholds were chosen (Figure 4b). The physically based hydrologic connectivity index was developed by integrating the indicator

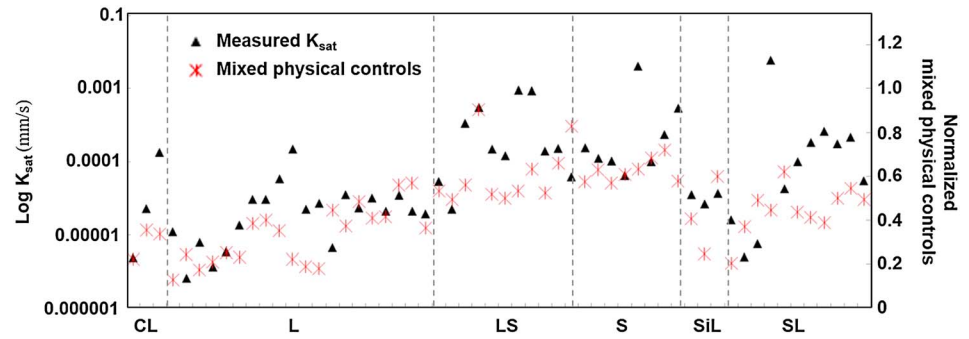


Figure 6. Comparison of spatial variations of measured saturated hydraulic conductivity (K_{sat}) and normalized mixed physical controls (%clay, %sand, NDVI, and TI) according to soil types across the LW watershed. CL: clay loam, L: loam, LS: loamy sand, S: sand, SiL: silty loam, and SL: sandy loam.

maps ranging from 1 to 5 ($\sum_{i=1}^5 I(y)_{s_i}$; s_i is the selected thresholds) (Figure 4c). Pixels of higher index represent fairly connected and higher wetness regions, while lower index pixels indicate unconnected and drier regions. The connectivity index was developed for each soil layer of CLM using the collected soil information with depth, NDVI, and TI and then used to calibrate soil hydraulic properties in land surface modeling. Cosby *et al.* [1984] developed a pedotransfer function for estimating soil hydraulic properties (θ_{sat} , K_{sat} , ψ_{sat} , and b) through a regression analysis using mean values of soil samples for various soil texture classes. The pedotransfer function has been applied in CLM to model the soil parameters as a set of default parameters. However, the default parameters might not be enough to successfully describe the soil moisture distribution in all areas/regions because they were derived from the texture-based mean values of soil samples collected across the conterminous U.S. Thus, in this study, we calibrated the parameters within their possible ranges (implying various characteristics of sample sites such as texture, topography, vegetation, among others) by accounting for their standard deviation obtained in Cosby *et al.* [1984] study (Table 2) ($P'_i = P_{i,def} \pm \alpha_i$). P'_i is the calibrated parameter set (θ_{sat} , ψ_{sat} , b , and K_{sat}); $P_{i,def}$ is the default parameter set; α_i is the calibrating factor for each parameter based on the standard deviation that is determined by the physically based hydrologic connectivity index. The value of α is added to the default

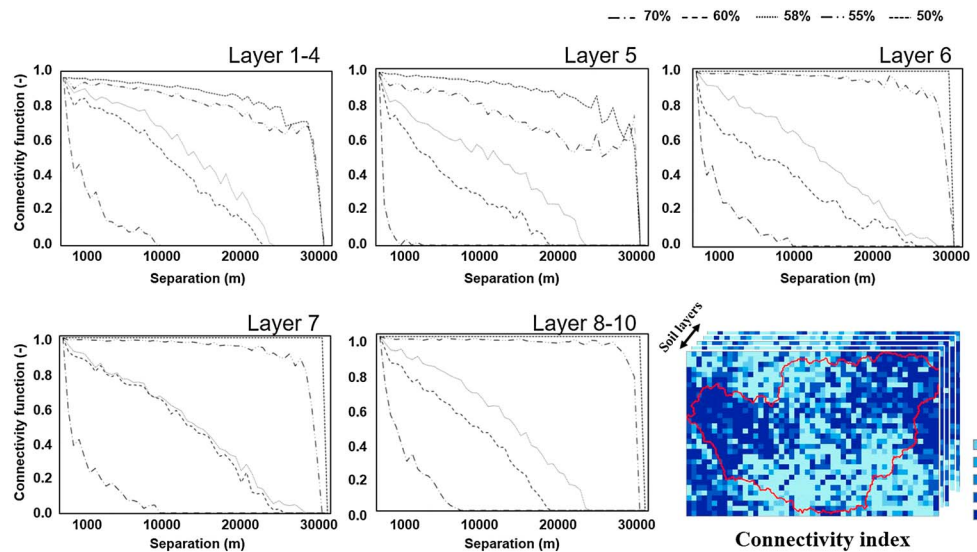


Figure 7. Connectivity functions for five representative thresholds for soil layers and connectivity index for the LW watershed. Pixels of higher index represent highly connected and higher wetness regions; lower index pixels indicate unconnected and drier regions.

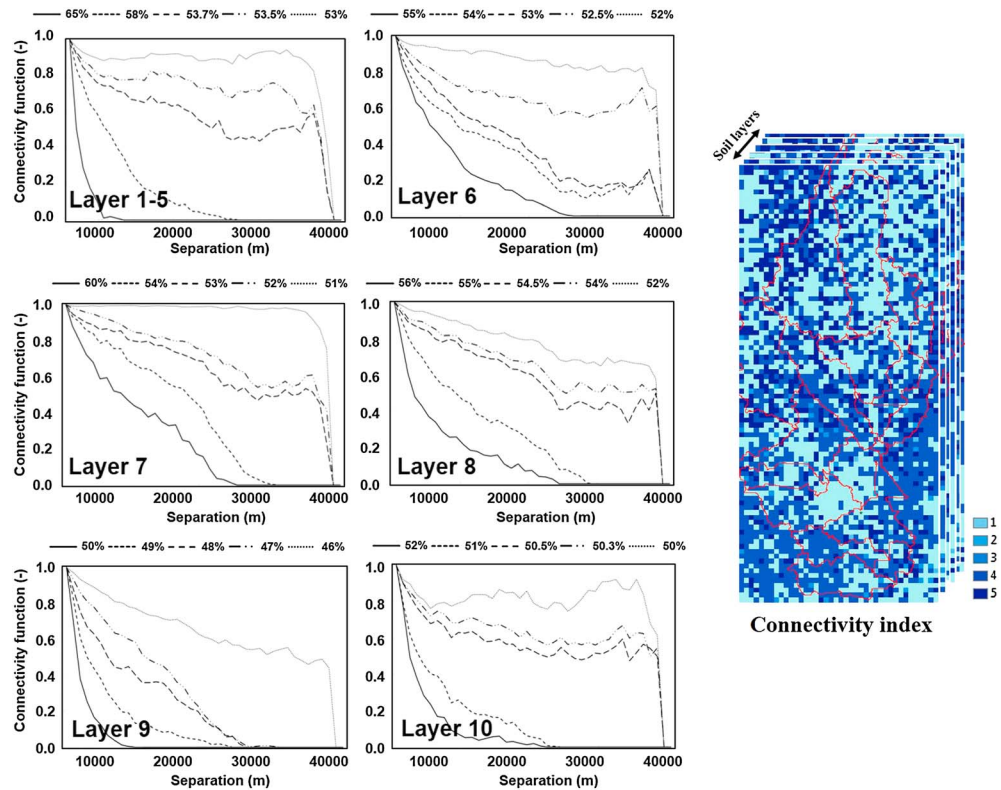


Figure 8. Connectivity functions for five representative thresholds for soil layers and connectivity index for the USS watershed. Pixels of higher index represent highly connected and higher wetness regions; lower index pixels indicate unconnected and drier regions.

soil parameters of θ_{sat} , ψ_{sat} , and b and subtracted from the parameter of K_{sat} when the connectivity index is greater than 3 representing connected regions of physical controls and higher soil water content; on the contrary, for other regions that have a connectivity index less than 3 reverse operation is performed. The calibrating factor was derived for each pixel across the domain as a constant value in time. The calibrated parameters based on physically based hydrologic connectivity were applied in CLM to effectively predict spatially distributed soil moisture. The model outputs using the default and calibrated parameters were compared to field observations.

3. Results and Discussions

In this study we investigated the effects of mixed dominant physical controls on soil moisture variability, developed the hydrologic connectivity algorithm to identify the spatial variations of soil moisture, and improved the parameterization of soil hydraulic properties. The proposed approach was tested in two watersheds (LW and USS) and compared to airborne remote sensing near-surface soil moisture data (800×800 m). The physically based hydrologic connectivity algorithm was applied to deeper soil layers as well as near-surface soil layer. However, we compared to near-surface observations only because of the lack of soil moisture information for deeper soils at watershed scales.

3.1. Effects of Mixed Physical Controls on Soil Moisture Variability

The contributing ratios of the most dominant controls (up to 4) were derived using the Bayesian averaging scheme. Figures 5a and 5b show the histograms of contributing ratios (w_1 , w_2 , w_3 , and w_4) of the physical controls (e.g., %clay, %sand, NDVI, and TI) for the two study sites. For the LW watershed, NDVI (w_3 of 0.438), %clay (w_1 of 0.326), and %sand (w_2 of 0.235) represented higher contributions to soil moisture spatial distribution, while topography seldom contributes at the support scale of 800×800 m (Figure 5a). The spatial distributions of soil texture and NDVI showed distinctive patterns across this watershed. The patterns indicated that the

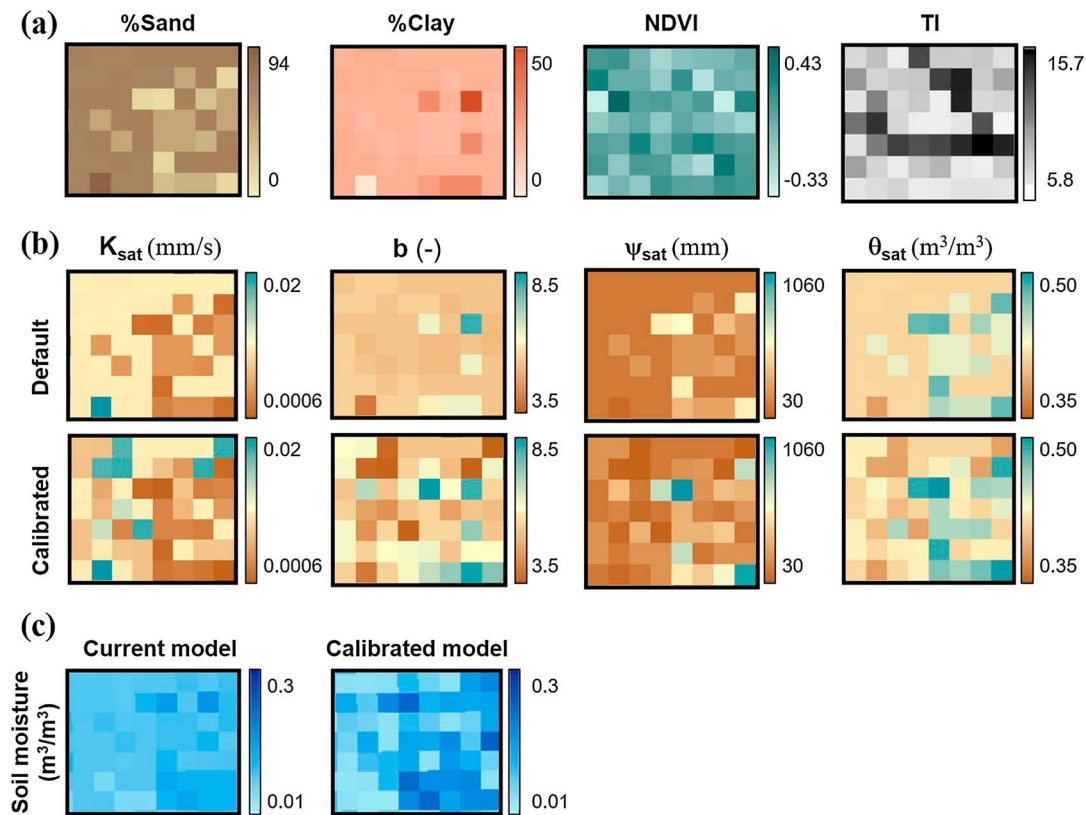


Figure 9. (a) Dominant physical controls, (b) default and calibrated soil hydraulic parameters, and (c) soil moisture prediction in the current (CLM) and calibrated model for a selected region (800×800 m resolution) in the LW watershed.

west and east parts of the watershed have higher values of %clay and NDVI and lower values of %sand corresponding to higher soil water content from ESTAR measurements. We also explored the effects of interactions between the physical controls (%clay · %sand, NDVI · %clay, NDVI · %sand, TI · %clay, TI · %sand, and NDVI · TI) on the contributions to soil moisture spatial variability. It was found that no significant contributions of the interactions existed in this watershed. It can be inferred that mixed response of individual physical controls based on their contributing ratios can predict the spatial variation of soil moisture well describing the distinctive patterns of landscape at the LW watershed. In addition, the spatial variation of mixed physical controls (normalized) was compared to the variability of measured saturated hydraulic conductivity (K_{sat}) from soil samples collected during the SGP97 hydrology experiment across the LW watershed. When K_{sat} measurements were rearranged according to soil types (CL = clay loam; L = loam; LS = loamy sand; S = sand; SiL = silty loam; and SL = sandy loam), it showed high variations even for the same soil types representing a similar tendency as the variation of mixed physical controls with higher contribution of NDVI (Figure 6). This could be caused by other coexisting physical controls such as vegetation cover which may affect soil water flow, because of root distribution and organic matter content leading to different pore size distribution and water holding capacity in the unsaturated zone.

For the USS watershed, we found that contributing ratios of the dominant controls estimated using the Bayesian averaging scheme tend to be biased toward soil texture (0.50 and 0.33 for %clay and %sand, respectively) with no significant contributions of NDVI and TI. As with the results of LW, the surface topography showed no valid contribution at this support scale (800×800 m). On the other hand, when the interaction terms between the dominant controls (%clay · %sand, NDVI · %clay, NDVI · %sand, TI · %clay, TI · %sand, and NDVI · TI) were included to account for the dependency of the physical controls, the interactions of %clay · NDVI and %sand · NDVI contributed significantly to the spatial distribution of soil moisture with resultant weights of 0.17 and 0.38, respectively (Figure 5b). It showed that NDVI influenced the description of the spatial variability of soil moisture as an interaction term with soil texture. In other words, the mixed effects of

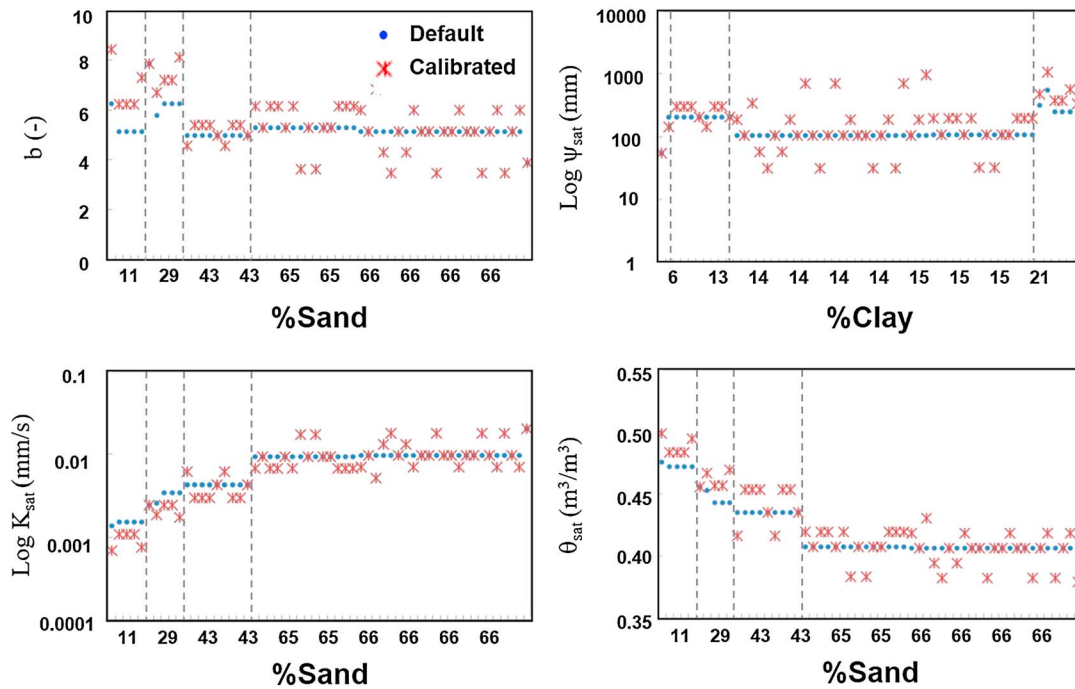


Figure 10. Comparisons of default and calibrated soil parameters according to soil texture (%sand and %clay). θ_{sat} , K_{sat} , and b are estimated based on %sand only; Ψ_{sat} is dependent on %clay only in pedotransfer function of CLM.

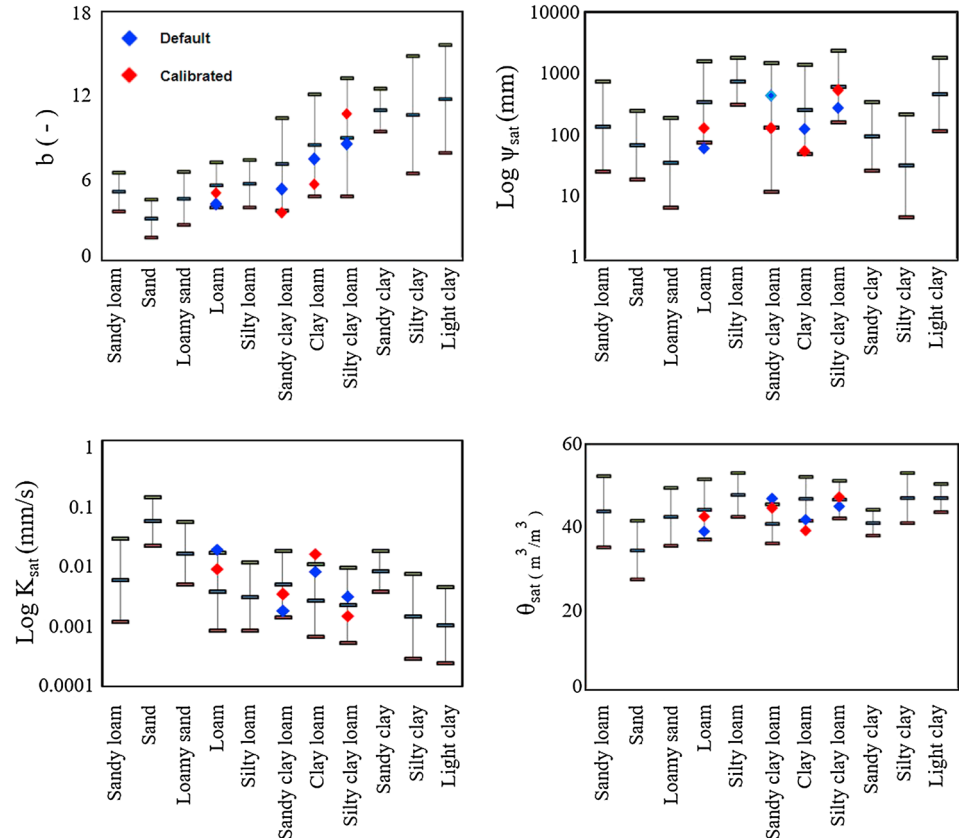


Figure 11. Comparison of default parameters and calibrated parameters on five selected pixels for the LW watershed. The bar shows the ranges of parameters for 11 soil texture classes obtained from Cosby *et al.* [1984].

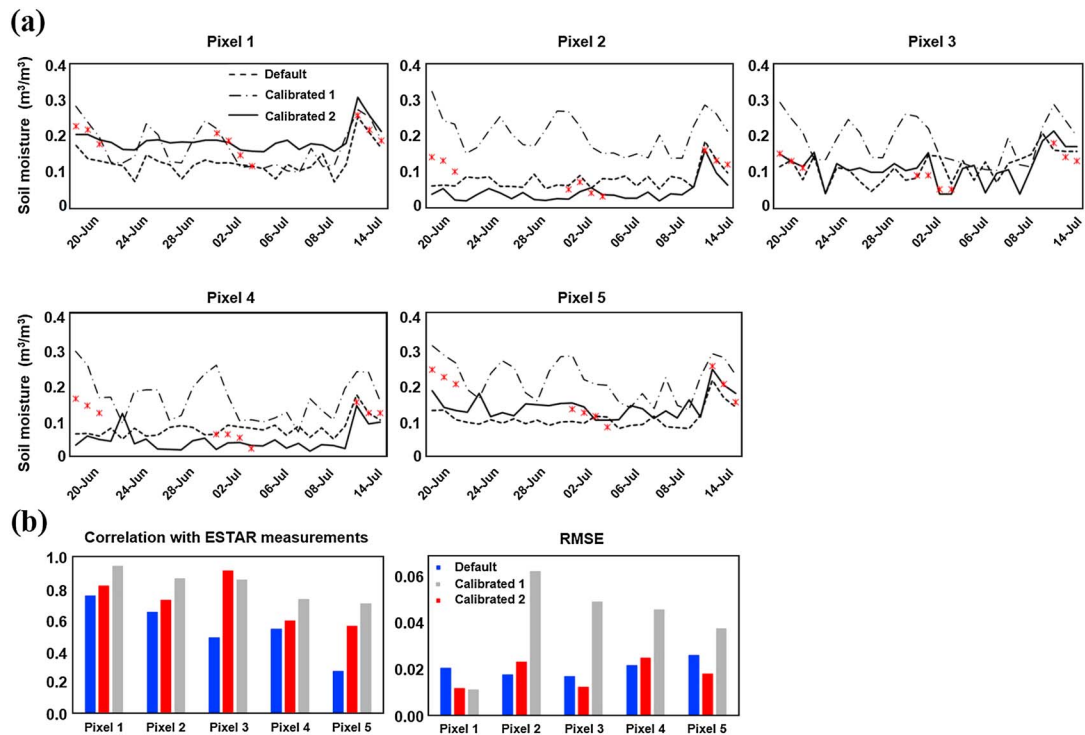


Figure 12. (a) Comparisons of simulated and measured soil moisture dynamics on 5 pixels selected on connected and unconnected regions and (b) correlation and RMSE with ESTAR measurements for 5 pixels in the LW watershed. Calibrated 1 and 2 represent model simulations using equal (proposed in Kim and Mohanty [2016]) and varied (proposed in this study) contributed ratios from physical controls, respectively.

interactions between physical controls as well as the individual controls on soil moisture distribution can be a characteristic feature of larger and complex landscapes such as USS and LW watersheds.

Thus, we mixed the spatial patterns of physical controls based on their contribution ratios (w_1 (%clay), w_2 (%sand), w_3 (NDVI), and w_4 (TI) for LW watershed; w_1 (%clay), w_2 (%sand), w_3 (NDVI·%clay), and w_4 (NDVI·%sand) for USS watershed) (Figures 5c and 5d) and developed hydrologic connectivity maps.

3.2. Calibration of Soil Hydraulic Properties Based On Hydrologic Connectivity

Since soil moisture measurements with depth are not available at watershed scales, the contributing ratios of physical controls derived from near-surface soil moisture were applied to combine the physical controls maps for deeper soil layers. Because connectivity functions can be different in different soil layers, the mixed physical controls map for each soil layer was created to calculate connectivity functions under various thresholds. The five representative thresholds (50%, 55%, 58%, 60%, and 70% for LW watershed and varying thresholds with depth for USS watershed) were found from connectivity functions for each soil layer that reflect connected patterns of the mixed physical controls well across the watersheds (Figures 7 and 8). Using the five thresholds, the indicator maps were generated, suggesting that the connectivity of mixed physical controls showed different patterns according to the thresholds which can reflect various spatial patterns of soil moisture in the unsaturated zone. In turn, the physically based hydrologic connectivity index was developed by adding the indicator maps and quantifying the soil moisture variability. The hydrologic connectivity index with soil depth was applied in calibrating the soil hydraulic properties in CLM, as depicted in Figure 2.

To analyze the spatial distributions of default and calibrated soil parameters, we selected a region which has complex landscape with relatively uniform soil types and heterogeneous vegetation cover and topography in the LW watershed. Figure 9 shows the comparison of spatial distributions of default and calibrated soil parameters. The default parameters have relatively uniform distributions depending on soil texture only (%sand and %clay) leading to low variation in soil moisture prediction. This is because CLM predicts soil hydraulic parameters from soil textural class alone. On the contrary, the parameters calibrated based on the physically based hydrologic connectivity index showed the spatially distributed patterns across the region.

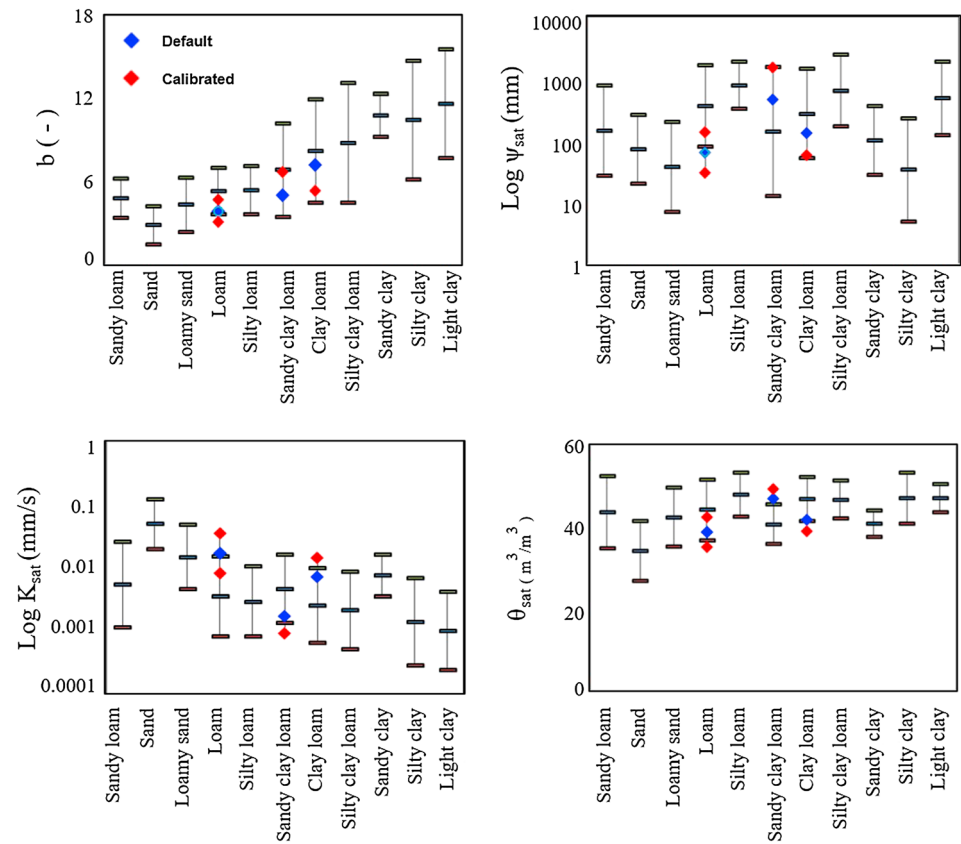


Figure 13. Comparison of default parameters and calibrated parameters on five selected pixels for the USS watershed. The bar shows the ranges of parameters for 11 soil texture classes obtained from Cosby et al. [1984].

Furthermore, the variations of default and calibrated soil hydraulic parameters were compared according to soil texture (Figure 10). The soil hydraulic parameters were uniformly predicted for the identical soil texture in the current model, while the calibrated parameters showed variations in space as shown in comparison of measured K_{sat} and mixed physical controls in Figure 6. Thus, the soil hydraulic parameters can be effectively calibrated using the hydrologic connectivity index to predict the variability of soil moisture in complex landscapes.

3.3. Comparison of CLM Output Using Default and Calibrated Soil Parameters

Model outputs (e.g., soil moisture, surface runoff, ET, and water storage) using the default and calibrated soil hydraulic properties were compared. Figure 11 shows the range of parameters based on their standard deviations in the Cosby et al. [1984] study. The default and calibrated parameters were compared for the selected 5 pixels (Figure 1) which have various soil texture classes (loam, sandy clay loam, clay loam, and silty clay loam) and different vegetation in the LW watershed. After calibrating the parameters based on the physically based hydrologic connectivity index, the soil parameters of b , θ_{sat} and ψ_{sat} were found to be higher than the default parameters and K_{sat} lower than its default values in pixels 1, 2, and 3 located on connected pixels in the connectivity index map. In contrast, it showed lower b , θ_{sat} , ψ_{sat} and higher K_{sat} for the calibrated parameters than those of the defaults in pixels 4 and 5 which are on unconnected pixels. Several default and calibrated parameters were out of the ranges of parameters because the parameters were estimated with the pedotransfer function derived through a regression analysis using mean values of soil samples. Using the calibrated parameters, the model can estimate higher soil water content in connected regions and lower soil water content in unconnected regions describing the spatially distributed soil moisture well across the LW watershed. Corroborating these findings, an improvement can be found by comparison of soil moisture dynamics on the selected pixels (Figures 12a and 12b). On pixels 1, 2, and 3 (connected pixels), the soil moisture dynamics simulated with the default parameters were underestimated, while the model simulation using

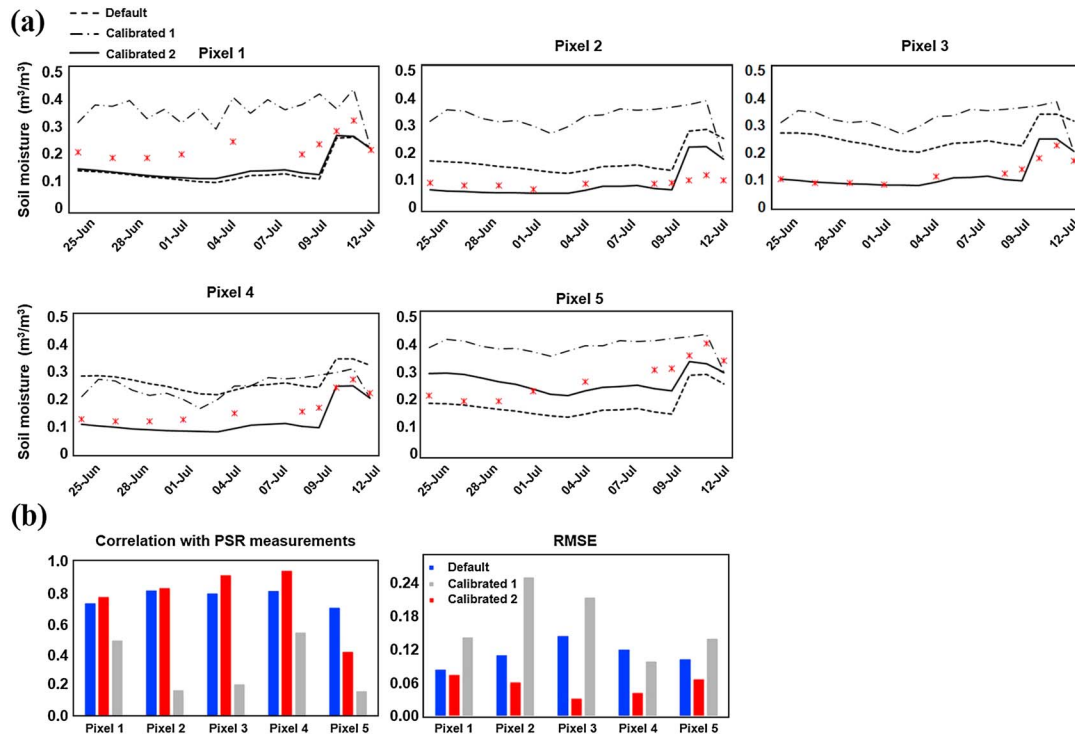


Figure 14. (a) Comparisons of simulated and measured soil moisture dynamics on 5 pixels selected on connected and unconnected regions and (b) correlation and RMSE with ESTAR measurements for 5 pixels in the USS watershed. Calibrated 1 and 2 represent model simulations using equal (proposed in *Kim and Mohanty* [2016]) and varied (proposed in this study) contributed ratios from physical controls, respectively.

the calibrated parameters showed good agreement with ESTAR measurements (correlation coefficient of 0.81, 0.72, and 0.91; RMSE of 0.028, 0.054, and 0.029 in Figure 12b). On the other hand, the current model using the default parameters overestimated the near-surface soil moisture on pixels 4 and 5 (unconnected pixels) compared to the measurements. The model prediction could be improved using the calibrated soil hydraulic parameters which match better with the measurements (correlation coefficient of 0.60 and 0.56; RMSE of 0.058 and 0.042 in Figure 12b) for the LW watershed. Furthermore, the model output using the varied contribution ratios from the physical controls (proposed in this study) was compared to that using the equal contribution ratios (proposed in *Kim and Mohanty* [2016]) as shown in Figure 12. It showed that the results from the previous concept could not effectively describe the spatial heterogeneity of soil moisture distribution.

For the USS watershed, we compared the default and calibrated parameters on the selected 5 pixels (Figure 13), which were plotted on the ranges of parameters for various soil texture classes. As discussed above, after calibrating the parameters based on the connectivity index, it showed higher values of b , θ_{sat} and ψ_{sat} and lower K_{sat} on pixels 1 (sand clay loam) and 5 (loam) which are on connected pixels compared to the default parameters. On the other hand, lower values of b , θ_{sat} and ψ_{sat} and higher K_{sat} were assigned to the unconnected pixels (2 (loam), 3 (loam), and 4 (clay loam)). When we compared the simulated soil moisture dynamics using the default and calibrated parameters on the selected pixels, the improvement of model performance was found (Figure 14a). Most of the pixels, except pixel 5, showed higher correlation with PSR measurements for the model output with the calibrated parameters, and RMSE was further reduced on all pixels (Figure 14b). In addition, the model predictions using the equal contributions of physical controls considerably overestimated soil moisture dynamics compared to that using the varied contributions and measurements. It can be inferred that we need to properly consider the spatial variability of physical controls to reflect landscape characteristics effectively in complex landscapes. Applying the calibrated parameters in land surface modeling, the parameters could make up for the default parameters' weaknesses which include underestimating the soil moisture dynamics on the connected regions and overestimating on the unconnected regions.

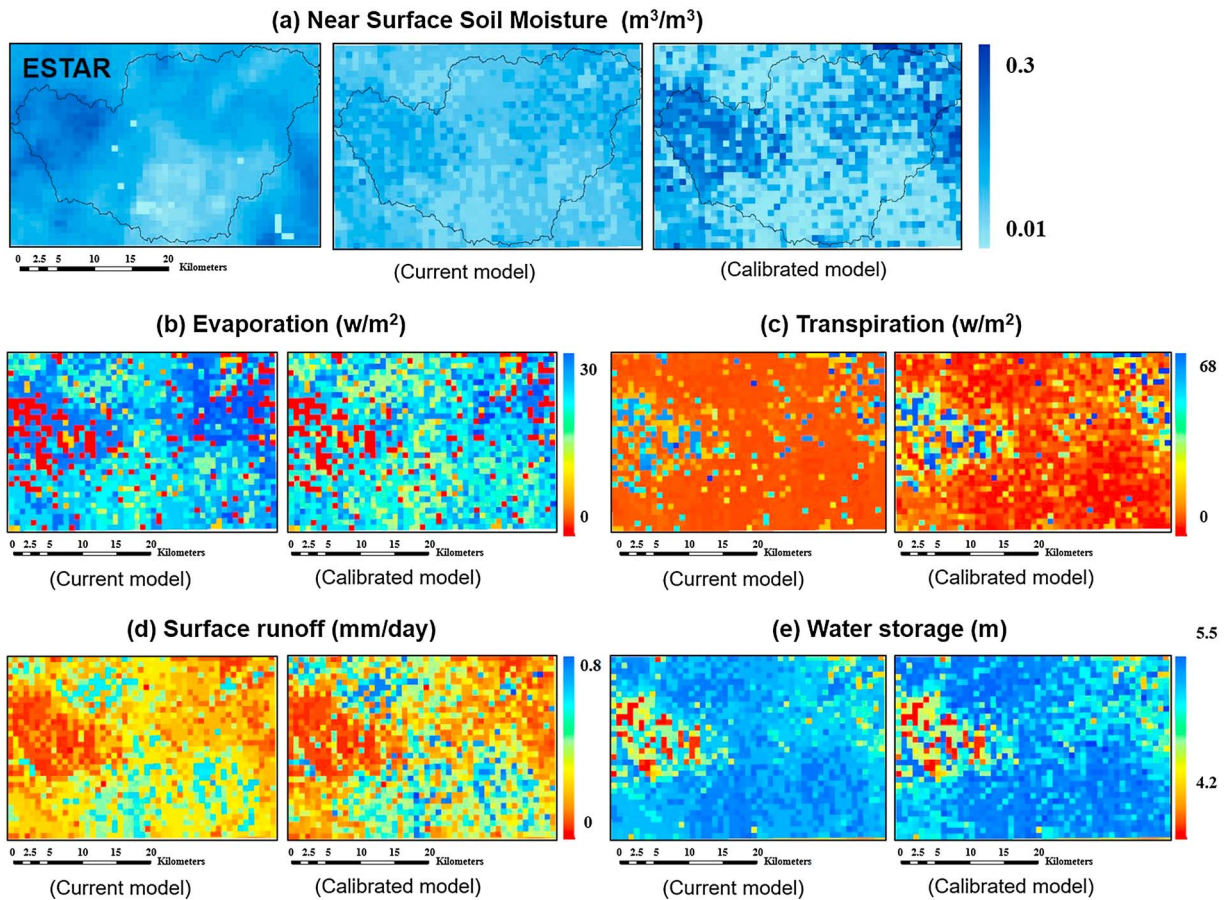


Figure 15. (a) Comparisons of measured and simulated soil moisture and (b–e) model outputs using default and calibrated parameters (evaporation, transpiration, surface runoff, and water storage) for the LW watershed.

Figures 15a and 16a show the comparisons of simulated near-surface soil moisture and ESTAR and PSR measurement for the entire watersheds. The simulated soil moisture using the default parameters tends to be underestimated in wet regions (connected pixels) and overestimated in dry regions (unconnected pixels). It could not capture the variability of soil moisture due to the default soil parameters related to soil textural class alone in the watersheds. The calibrated model simulation matched well with the measurements (ESTAR and PSR) showing higher and lower soil water content on the connected and unconnected pixels, respectively. The spatial variability of soil moisture prediction was compared at various extent scales. Table 3 shows the correlation coefficients and RMSE between measured soil moisture and model simulation (top 5 cm) using the default and calibrated soil parameters for different extent scales within the watersheds. At all extent scales the calibrated model showed higher correlation coefficients (0.310–0.713 for LW and 0.400–0.712 for USS) and lower RMSE (0.016–0.048 for LW and 0.081–0.099 for USS) than that of the current model that represented improvements of model performance in space. Thus, the spatial variations of soil moisture can be properly described using soil parameters calibrated by physically based hydrologic connectivity. Consequentially, these differences between the current and calibrated models can lead to different model outputs (e.g., root zone soil moisture, evapotranspiration, surface runoff, and water storage) as shown in Figures 15b–15e and 16b–16d that could have important effects not only on water cycle but also on surface energy budgets.

Based on these findings, the physically based hydrologic connectivity developed in this study helped to better understand the spatial variability of soil moisture in the unsaturated zone. Furthermore, the model performance using the calibrated soil hydraulic parameters based on the connectivity index was improved compared to the model predictions using the default parameters. It can be inferred that soil hydraulic parameters calibrated with physically based hydrologic connectivity can efficiently reflect the variations of soil moisture in space in land surface modeling at regional scales.

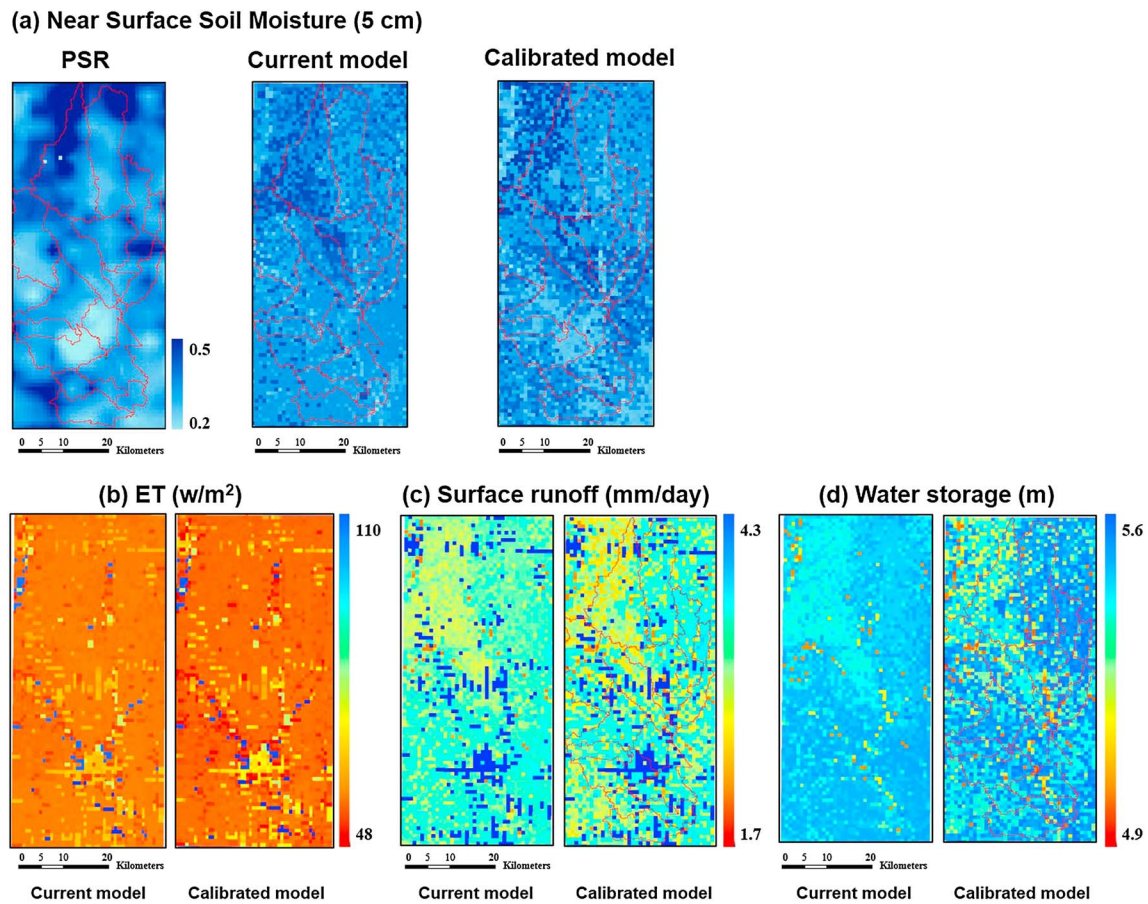


Figure 16. (a) Comparisons of measured and simulated soil moisture and (b–d) model outputs using default and calibrated parameters (ET, surface runoff, and water storage) for the USS watershed.

4. Summary and Conclusions

In this study, we developed a physically based hydrologic connectivity algorithm to better understand catchment hydrologic characteristics and identify the soil moisture variability. To develop hydrologic connectivity based on dominant physical controls, the effects of mixed physical controls (e.g., topography, soil texture, and vegetation) jointly on soil moisture spatial distribution were investigated at two different hydroclimate regions (subhumid and humid climate). The physical controls can similarly contribute to describing the spatial variability of soil moisture in some regions as shown in *Kim and Mohanty* [2016], but it can also vary with complex landscape characteristics. Thus, the previous methodology [*Kim and Mohanty*, 2016] works well in a

Table 3. Correlation Coefficients and RMSE Between Soil Moisture Measurements and Simulations (Top 5 cm) Using Default and Calibrated Soil Parameters for the Two Study Sites

	LW				USS			
	2×7^a	4×9^a	8×13^a	12×15^a	24×4^a	32×7^a	36×11^a	40×15^a
	<i>R</i>							
Default	0.164	0.250	0.540	0.669	0.512	0.389	0.371	0.237
Calibrated	0.310	0.452	0.674	0.713	0.712	0.587	0.488	0.400
	<i>RMSE</i>							
Default	0.048	0.047	0.051	0.050	0.128	0.123	0.115	0.102
Calibrated	0.016	0.044	0.048	0.047	0.099	0.098	0.090	0.081

^aNumber of pixels (extent scale) = 1.6×1.6 km resolution; extent scales were determined by the shape of watersheds.

certain region or does not work in other regions. That is why we improved the methodology with varied contribution ratios in this study. Using the Bayesian averaging scheme, the contributing ratios of physical controls to soil moisture distribution were derived to combine the controls for the two study sites. In the LW site, soil texture (%clay and %sand) and vegetation (NDVI) showed higher contributions and no significant contributions of interactions between the controls existed. On the other hand, soil texture and the interactions between vegetation and soil texture represented valid contributions to spatial patterns of soil moisture in the USS site. We found that the contributing ratios of physical controls could be site specific depending on landscape characteristics, and the interaction terms of physical controls could also affect soil moisture distribution. Based on the contributing ratios, the dominant physical controls were combined and used for developing hydrologic connectivity using the integral connectivity scale technique. In order to identify the connectivity, we generated indicator maps using various thresholds selected from the connectivity functions. In turn, the physically based hydrologic connectivity index was developed by aggregating the indicator maps representing the connected (wet regions) and unconnected (dry regions) patterns across the watersheds, which can properly describe the soil moisture spatial variability.

The hydrologic connectivity index was applied in calibrating soil hydraulic properties (θ_{sat} , K_{sat} , ψ_{sat} , and b) to improve the current parameterization in land surface modeling (CLM). When we compared the simulated soil moisture using the default and calibrated parameters to remote sensing measurements (ESTAR and PSR), the calibrated model simulation showed good agreement with the measurements. The simulated soil moisture dynamics on selected pixels were improved with the calibrated parameters indicating higher soil moisture prediction on the connected pixels and lower prediction on the unconnected pixels. Thus, using the physically based hydrologic connectivity, we could describe the spatial patterns of soil moisture and improve the current parameterization and model performance. Based on these results, the differences in model outputs using the default and calibrated soil parameters could have important effects not only on water cycle but also on surface energy budgets. In general application, the physically based hydrologic connectivity index can be applicable to other regions which have similar patterns of dominant physical controls for developing hydrologic connectivity using identical thresholds. Furthermore, land surface models at the global scale currently use averaged soil parameters in a pixel, which could not reflect the spatial variability of soil properties in a large area (a pixel). To overcome the limitation, the proposed approach can be applied for deriving effective soil properties based on hydrologically connected patterns of physical controls. In addition, remotely sensed soil moisture products (e.g., AMSR-E, SMOS, and SMAP) can be used for determining the contributions of physical controls at the global scale. For future work, since hydrologic connectivity patterns can vary with time, a dynamic connectivity index can be considered in the parameterization scheme to account for temporal variability of soil moisture in the unsaturated zone and improve model performance for long-term simulations.

Acknowledgments

This research was funded by NASA THP-NNX09AK73G grant. ESTAR and PSR remote sensing footprint used in this study were collected from Southern Great Plains experiment 1997 (SGP97, contact person: Michael H. Cosh (michael.cosh@ars.usda.gov) at USDA-ARS Hydrology and Remote Sensing Lab) and Soil Moisture Experiment 2002 (SMEX02, http://nsidc.org/data/amsr_validation/soil_moisture/smex02/index.html), respectively. Weather data sets were obtained from USDA Agricultural Research Service (ARS) Micronet (<http://ars.mesonet.org/webrequest/>) and SMEX02 Rain Gauge network (http://nsidc.org/data/amsr_validation/soil_moisture/smex02/index.html), respectively. The required input data sets (land cover, soil types, and topographic information) were collected from NLCD (National Land Cover Database, <http://www.mrlc.gov/>), SSURGO (Soil Survey Geographic database, http://www.nrcs.usda.gov/wps/portal/nrcs/detail/soils/survey/geo/?cid=nrcs142p2_053631), and NED (National Elevation Dataset, <http://ned.usgs.gov/>), respectively.

References

- Ali, G. A., and A. G. Roy (2009), Revisiting hydrologic sampling strategies for an accurate assessment of hydrologic connectivity in humid temperate systems, *Geogr. Compass*, 3(1), 350–374, doi:10.1111/j.1749-8198.2008.00180.x.
- Ali, G. A., and A. G. Roy (2010), Shopping for hydrologically representative connectivity metrics in a humid temperate forested catchment, *Water Resour. Res.*, 46, W12544, doi:10.1029/2010WR009442.
- Amoros, C., and G. Bornette (2002), Connectivity and biocomplexity in waterbodies of riverine floodplains, *Freshwater Biol.*, 47(4), 761–776.
- Bindlish, R. and T. J. Jackson (2002), *SMEX02 Aircraft Polarimetric Scanning Radiometer (PSR) Data*. [indicate subset used]. Boulder, Colorado USA: NASA National Snow and Ice Data Center Distributed Active Archive Center., doi: 10.5067/4N9BFV091ZXH.
- Bonan, G. B. (1996), A land surface model (LSM version 1.0) for ecological, hydrological, and atmospheric studies: Technical description and user's guide NCAR Tech. Note NCAR/TN-417+STR, pp. 150.
- Clapp, R. B., and G. M. Hornberger (1978), Empirical equations for some soil hydraulic properties, *Water Resour. Res.*, 14(4), 601–604, doi:10.1029/WR014i004p00601.
- Cosby, B. J., G. M. Hornberger, R. B. Clapp, and T. R. Ginn (1984), A statistical exploration of the relationship of soil moisture characteristics to the physical properties of soils, *Water Resour. Res.*, 20(6), 682–690, doi:10.1029/WR020i006p00682.
- Dickinson, R. E., A. Henderson-Sellers, and P. J. Kennedy (1993), Biosphere atmosphere transfer scheme (BATS) version 1e as coupled to the NCAR Community Climate Model *NCAR Tech. Note, NCAR/TN-378 + STR*, Natl. Cent. For Atmos. Res., Boulder, Colo.
- Emanuel, R. E., A. G. Hazen, B. L. McGlynn, and K. G. Jencso (2014), Vegetation and topographic influences on the connectivity of shallow groundwater between hillslopes and streams, *Ecology*, 7, 887–895.
- Famiglietti, J., J. Devereaux, C. A. Laymon, T. Tsegaye, P. R. Houser, T. J. Jackson, S. T. Graham, M. Rodell, and P. J. van Oevelen (1999), Ground-based investigation of soil moisture variability within remote sensing footprints during the Southern Great Plains 1997 (SGP 97) Hydrology Experiment, *Water Resour. Res.*, 35(6), 1839–1851, doi:10.1029/1999WR000047.
- Gaur, N., and B. P. Mohanty (2013), Evolution of physical controls for soil moisture in humid and subhumid watersheds, *Water Resour. Res.*, 49, 1244–1258, doi:10.1002/wrcr.20069.

- Gaur, N., and B. P. Mohanty (2016), Land-surface controls on near-surface soil moisture dynamics: Traversing remote sensing footprints, *Water Resour. Res.*, *52*, doi:10.1002/2015WR018095.
- Hoetting, J. A., D. Madigan, A. E. Raftery, and C. T. Volinsky (1999), Bayesian modeling averaging: A tutorial, *Stat. Sci.*, *14*(4), 382–417.
- Huang, M., Z. Hou, L. R. Leung, Y. Ke, Y. Liu, Z. Fang, and Y. Sun (2013), Uncertainty analysis of runoff simulations and parameter identifiability in the community land model: Evidence from MOPEX basins, *J. Hydrometeorol.*, *14*, 1754–1772, doi:10.1175/JHM-D-12-0138.1.
- Hwang, T., L. Band, and T. C. Hales (2009), Ecosystem processes at the watershed scale: Extending optimality theory from plot to catchment, *Water Resour. Res.*, *45*, W11425, doi:10.1029/2009WR007775.
- Jackson, T. J., D. M. Le Vine, A. Y. Hsu, A. Oldak, P. J. Starks, C. T. Swift, J. D. Isham, and M. Haken (1999), Soil moisture mapping at regional scales using microwave radiometry: The Southern Great Plains hydrology experiment, *IEEE Trans. Geosci. Remote Sens.*, *37*, 2136–2151.
- Jencso, K. G., and B. L. McGlynn (2011), Hierarchical controls on runoff generation: Topographically driven hydrologic connectivity, geology, and vegetation, *Water Resour. Res.*, *47*, W11527, doi:10.1029/2011WR010666.
- Jencso, K. G., B. L. McGlynn, M. N. Gooseff, S. M. Wondzell, K. E. Bencala, and L. A. Marshall (2009), Hydrologic connectivity between landscapes and streams: Transferring reach- and plot-scale understanding to the catchment scale, *Water Resour. Res.*, *45*, W04428, doi:10.1029/2008WR007225.
- Jencso, K. G., B. L. McGlynn, M. N. Gooseff, K. E. Bencala, and S. M. Wondzell (2010), Hillslope hydrologic connectivity controls riparian groundwater turnover: Implications of catchment structure for riparian buffering and stream water sources, *Water Resour. Res.*, *46*(11), W10524, doi:10.1029/2009WR008818.
- Joshi, C., and B. P. Mohanty (2010), Physical controls of near surface soil moisture across varying spatial scales in an agricultural landscape during SMEX02, *Water Resour. Res.*, *46*, W12503, doi:10.1029/2010WR009152.
- Kim, J., and B. P. Mohanty (2016), Influence of lateral subsurface flow and connectivity on soil water storage in land surface modeling, *J. Geophys. Res. Atmos.*, *121*, 704–721, doi:10.1002/2015JD024067.
- Knudby, C., and J. Carrera (2005), On the relationship between indicators of geostatistical, flow and transport connectivity, *Adv. Water Resour.*, *28*, 405–421.
- Larsen, L. G., J. Choi, M. K. Nungesser, and J. W. Harvey (2012), Direction connectivity in hydrology and ecology, *Ecol. Appl.*, *22*(8), 2204–2220.
- Li, H., M. Huang, M. S. Wigmosta, Y. Ke, A. M. Coleman, L. R. Leung, A. Wang, and D. M. Ricciuto (2011), Evaluating runoff simulations from the Community Land Model 4.0 using observations from flux towers and a mountainous watershed, *J. Geophys. Res.*, *116*, D24120, doi:10.1029/2011JD016276.
- Mayor, Á. G., S. Bautista, E. E. Small, M. Dixon, and J. Bellot (2008), Measurement of the connectivity of runoff source areas as determined by vegetation pattern and topography: A tool for assessing potential water and soil losses in drylands, *Water Resour. Res.*, *44*, W10423, doi:10.1029/2007WR006367.
- McDonnell, J. J., et al. (2007), Moving beyond heterogeneity and process complexity: A new vision for watershed hydrology, *Water Resour. Res.*, *43*, W07301, doi:10.1029/2006WR005467.
- McGarigal, K., S. A. Cushman, M. C. Neel, and E. Ene (2002), *FRAGSTATS: Spatial Pattern Analysis Program for Categorical Maps*, Univ. of Massachusetts, Amherst, Mass. [Available at <http://www.umass.edu/landeco/research/fragstats/fragstats.html>.]
- Mohanty, B. P., and T. H. Skaggs (2001), Spatio-temporal evolution and time-stable characteristics of soil moisture within remote sensing footprints with varying soil, slope, and vegetation, *Adv. Water Resour.*, *24*, 1051–1067.
- Moore, I. D., P. E. Gessler, G. A. Nielsen, and G. A. Peterson (1993), Soil attribute prediction using terrain analysis, *Soil Sci. Soc. Am. J.*, *57*(2), 443–452.
- Niu, G.-Y., Z.-L. Yang, R. E. Dickinson, and L. E. Gulden (2005), A simple TOPMODEL-based runoff parameterization (SIMTOP) for use in GCMs, *J. Geophys. Res.*, *110*, D21106, doi:10.1029/2005JD006111.
- Niu, G.-Y., Z.-L. Yang, R. E. Dickinson, L. E. Gulden, and H. Su (2007), Development of a simple groundwater model for use in climate models and evaluation with Gravity Recovery and Climate Experiment data, *J. Geophys. Res.*, *112*, D07103, doi:10.1029/2006JD007522.
- Oleson, K. W., D. M. Lawrence, G. B. Bonan, M. G. Flanner, E. Kluzek, P. J. Lawrence, S. Levis, S. C. Swenson, and P. E. Thornton (2010), Technical description of version 4.0 of the Community Land Model (CLM) NCAR Tech. Notes (NCAR/TN-478+STR), 257 pp.
- Phillip, J. R., and D. de Vries (1957), Moisture movement in porous materials under temperature gradients, *Trans. Am. Geophys. Union*, *38*, 222–232.
- Price, K., C. R. Jackson, and A. J. Parker (2010), Variation of surficial soil hydraulic properties across land uses in the southern Blue Ridge Mountains, North Carolina, USA, *J. Hydrology*, *383*, 256–268.
- Ricotta, C., A. Stanisci, G. C. Avena, and C. Blasi (2000), Quantifying the network connectivity of landscape mosaics: A graph-theoretical approach, *Community Ecol.*, *1*, 89–94.
- Sivapalan, M. (2005), Pattern, process and function: Elements of a unified theory of hydrology at the catchment scale, in *Encyclopedia of Hydrological Sciences*, edited by M. G. Anderson, pp. 193–220, John Wiley, Chichester, U. K.
- Smith, T., L. Marshall, B. McGlynn, and K. Jencso (2013), Using field data to inform and evaluate a new model of catchment hydrologic connectivity, *Water Resour. Res.*, *49*, 6834–6846, doi:10.1029/wrcr.20130546.
- Western, A. W., G. Bloschl, and R. B. Grayson (1998), How well do indicator variograms capture the spatial connectivity of soil moisture?, *Hydrol. Process.*, *12*, 1851–1868.
- Western, A. W., R. B. Grayson, G. Bloschl, G. R. Willgoose, and T. A. McMahon (1999), Observed spatial organization of soil moisture and its relation to terrain indices, *Water Resour. Res.*, *35*(3), 797–810, doi:10.1029/1998WR900065.
- Western, A. W., G. Bloschl, and R. B. Grayson (2001), Toward capturing hydrologically significant connectivity in spatial patterns, *Water Resour. Res.*, *37*, 83–97, doi:10.1029/2000WR900241.
- Western, A. W., S. Zhou, R. B. Grayson, T. A. McMahon, G. Bloschl, and D. J. Wilson (2004), Spatial correlation of soil moisture in small catchments and its relationship to dominant spatial hydrological processes, *J. Hydrology*, *286*, 113–134.
- Wilson, D. J., A. W. Western, and R. B. Grayson (2005), A terrain and data-based method for generating the spatial distribution of soil moisture, *Adv. Water Resour.*, *28*(1), 43–54.
- Zeng, X. B., and M. Decker (2009), Improving the numerical solution of soil moisture-based Richards equation for land models with a deep or shallow water table, *J. Hydrometeorol.*, *10*, 308–319.
- Zhu, Q., and H. S. Lin (2010), Comparing ordinary kriging and regression kriging for soil properties in contrasting landscapes, *Pedosphere*, *20*(5), 594–606.